CRACK PROPAGATION IN MARITIME PINE BEAMS UNDER HUMIDITY VARIATIONS: COHESIVE CRACK METHOD

Ngoc Anh Phan[1], Myriam Chaplain[2], Stéphane Morel[3], Jean-Luc Coureau[4]

ABSTRACT: The aim of this work is to predict the crack propagation in wood beams under climate conditions. This work is based on Linear Elastic Mechanics equivalent Rupture. A model is developed in the finite element (FE) code Cast3M; it is based on the theory of a cohesive crack and takes into account the influence of moisture content on the fracture process zone. Monotonous fracture tests in mode I are performed on the Maritime pine under different moisture contents in order to determine cohesive zone model parameters (bilinear softening law). Fracture tests under constant load are also performed under relative humidity variations. In addition, mass transfer is integrated in the modelling to determine the moisture content at all points of the mesh as a function of humidity. The mecanosorptive behaviour of wood is also introduced in the FE calculations. The simulation has been validated by comparison with experimental results.

KEYWORDS: crack propagation, cohesive zone model, moisture content, diffusion, mecanosorption, Maritime pine

1 INTRODUCTION

In recent years, the wood construction has achieved a large success in the world due to the environmental and ecological context. However, the lifetime of the structure is affected by climate change. Climate change (such as variation of relative humidity, temperature) causes development of cracks in structural elements (i.e., beam, column...) and reduces the lifetime of this structure.

Wood beams with defaults such as notches or tapered end-notches, which causes stress concentrations, are greatly influenced by relative humidity variation. With the presence of large stress gradients, the propagation of a crack or cracks leads to the failure. Therefore, the issue of the moisture content impact on the fracture properties as well as the process of crack growth in wood material begins to gain more attention tin the studies.

In the fracture mechanics approach, cohesive zone models have been widely employed in order to describe the fracture behaviour in wood. The cohesive zone represents the small fracture process zone (FPZ) ahead the crack tip and its behaviour can be defined by a traction-separation law [3]. Varying RH induces internal stresses which may cause the crack propagation because the FPZ at the crack tip is directly submitted to relative humidity variations [4].

In this research, we focus on the moisture influence on the fracture process zone during the crack propagation.

2 EXPERIMENTS

Fracture tests in mode I have been frequently carrying out on different specimen types, most of them on Double Cantilever Beam (DCB). Under tests on DCB, the energy release rate increases in function of the crack length. Undoubtedly, this evolution depends on the specimen geometry: this is why an inclined profile of the DCB specimen - called Tapered Double Cantilever Beam (TDCB) - is interesting and suitable in the mentioned context [4]. In this work, fracture tests are carrying out on modified Tapered Double Cantilever Beam (mTDCB). Figure 1 presents the geometry and dimensions of the tested specimen. The mTDCB geometry provides a stable crack growth when the crack is in the inclined zone 1. The specimen dimensions assure quasi-constant force in the post-pic regime during the monotonic test. Thanks to these stability, creep tests under humidity variation can be performed. The crack evolution will only depend on MC variations and on viscosity. If the sizes of a specimen are greater than these dimensions the creep tests cannot be carried out due to the limit of the experimental laboratory equipment such as the climatic chamber, the imposed load level...

Fracture tests in mode I are carrying out on TL configuration (L is the direction of the crack propagation; T is the load direction) on Maritime pine specimens [12-13]. The initial crack length (a_0= 40 mm) is machined with a band saw (thickness 1 mm) and prolonged a few millimetres with a sharp blade which is sliced along the notch tip to initiate the crack. The crack

[1] Ngoc Anh Phan, University of Bordeaux, I2M/GCE, 351 cours de la libération-33405 Talence cedex France
[2] Myriam Chaplain, University of Bordeaux, I2M/GCE, 351 cours de la libération-33405 Talence cedex France – myriam.chaplain@u-bordeaux.fr
[3] Stéphane Morel, University of Bordeaux, I2M/GCE, 351 cours de la libération-33405 Talence cedex France
[4] Jean-Luc Coureau, University of Bordeaux, I2M/GCE, 351 cours de la libération-33405 Talence cedex France

front alignment is verified by measuring the initial crack length on both sides of the specimen.
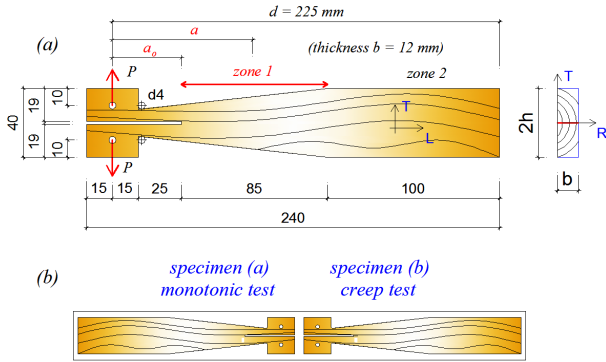

Figure 1: Dimension of the mTDCB specimen (a); cutting position of mTDCB for two fractures tests

Two different fracture tests in mode I at a wide range of moisture contents have been realised:
- monotonic (quasi-static) tests under different MC in order to determine the strength (maximal load), the cohesive zone model parameters.
- creep tests under RH variation in order to investigate the fracture response of the material under the humidity variation.

Furthermore, specimens used in the two different fracture tests are twin extracted from the same piece of wood (Figure 1) to assure more similar properties between them. The strength of the specimen (b) is supposed to be the same as the one of specimen (a). Hence, the strength of the specimen (a) is used to determine the stress level applied to the specimens (b) during the creep test.

2.1 Monotonic tests under different moisture contents

Firstly, monotonous fracture tests are carried out on nearly 300 specimens at 10 MC conditions (5%, 8%, 10%, 12%, 15%, 18%, 20%, 22%, 25% and 30%). Each specimen is stored into climatic boxes under constant temperature (20°C) and relative humidity corresponding to the expected moisture. Before and after the test, the mass and the dimensions of each specimen are measured. The moisture loss during test is small and its effects are negligible. In order to minimize the visco-elastic effects and to avoid the change of the moisture content during tests, the complete fracture of a specimen is obtained in 3 min: the displacement velocity is 1 mm/min for MC lower than 22% MC and 2 mm/min for higher 22% MC.

During experimental tests, load/displacement data has been recorded to calculate the fracture energy (acquisition frequency of 10 Hz). Load displacement has been recorded using a camera (Figure 2). From this system, we follow the displacements of the two loading points P1, P2 and of two other points O1, O2 which give the evolution of the crack opening displacement.
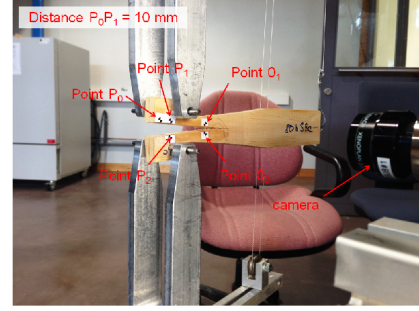

Figure 2: Experimental setup for monotonic fracture test

The Figure 3 presents typical load displacement curves obtained for 3 moisture content (MC). The maximum load decreases when the moisture increases.
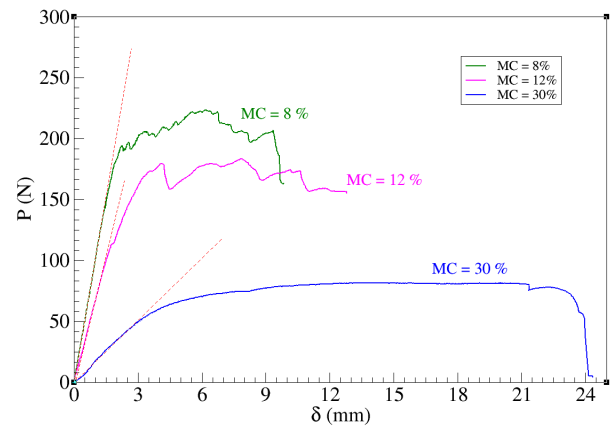

Figure 3: Typical load-displacement curves at 3 moisture MC

At the begin of the loading, some short cracks appear around the crack tip due to a singular stress; when this stress reaches the tensile strength, fibers presenting short cracks are damaged and deformed but not broken. Through the damaged but not yet broken fibers around the crack tip, the stress can be transferred from the upper to the lower parts of the specimen but the transfer decreases when the deformation of the fibers increases. The stress transfer establishes an initial softening zone (FPZ) in the vicinity of the crack tip (Figure 4). On the other hand, the description of the last phenomenon corresponds to the same concept of the cohesive theory. We consider that the short cracks exist in the micro-cracking zone (Figure 4). When the load increases, the short crack will be more developed and fibers are more damaged. The fibers deformation level depends on the mechanical properties of wood. At this state, two different damaged zones exist: the micro-cracking and the fiber bridging zone (or macro-cracking zone) (Figure 4). In reality, even with recent adapted methods such as the digital image correlation technical (DIC), the topographic technical or with the criterion based on the width of short crack, we still do not have a feasible and robust method to clearly distinguish these two zones in experimental tests. Nevertheless, we can overcome this difficulty thanks to the bi-linear function where the separation of two zones is described by the cohesive energy ratio $G_{f\mu}/G_f$ developed in Section 3.
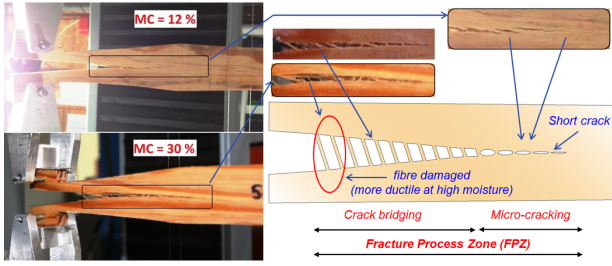
Figure 4: *crack growth mechanism in wood versus MC: crack bridging and micro cracking*

2.2 Creep tests: crack propagation under RH variations

Secondly, specimens are subjected to constant load under variable relative humidity conditions at constant temperature (20°C). The RH varies from 40% to 90% per 12 hours cycles. This RH variation corresponds nearly to 7% to 22% moisture variation at the specimen surface. The initial (conditioned) moisture of the specimens were around 12%.

A digital camera is also employed to follow the evolution of the loading point displacement and of the crack opening displacement of specimen during the creep test (1 image every 10 min) (Figure 5).
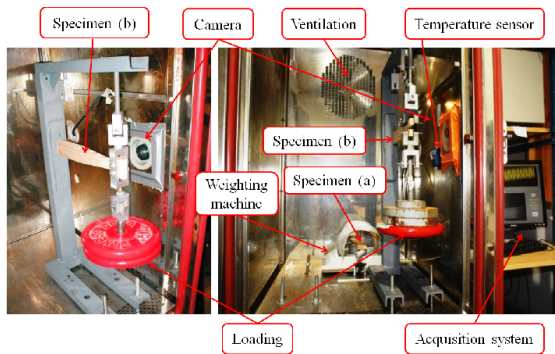

Figure 5: *Experimental setup for creep tests inside the climatic chamber*

These creep tests will allow us to describe more precisely the effect of climate conditions and its variations on the delayed fracture.

3 COHESIVE ZONE MODEL

In the present work, a bilinear softening function in the traction-separation law is used to describe the quasi-brittle fracture of wood at different moisture contents. The shape of this function plotted in Figure 6 is characterized by 4 parameters: the cohesive fracture energy G_f (J/m^2), the critical opening w_c (mm), the tensile strength f_t (MPa) and the energy distribution (characterized by the ratio $G_{f\mu}/G_f$).
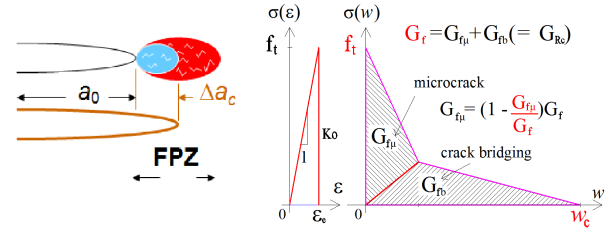

Figure 6: *Schematic representation of the Fracture Process Zone (FPZ) and of bilinear softening function*

An estimation procedure proposed by Morel et al. [5, 13-14], based on the equivalent LEFM R-curve, is used to obtain the 4 CZM parameters from monotonous tests at 10 moisture contents. Parameters of the bi-linear softening law are summarized in Table 1 for all moisture contents.

Table 1: *Cohesive parameters at 10 MC: mean values and standard deviation in brackets*

MC (%)	Number of specimens	G_f (J/m^2)	w_c (mm)	f_t (MPa)	$G_{f\mu}/G_f$
4.96	28	477	0.27	6.21	0.630
(0.35)		(58)	(0.10)	(0.40)	(0.033)
7.93	20	503	0.38	5.18	0.618
(0.38)		(62)	(0.09)	(0.38)	(0.048)
9.89	31	538	0.57	4.40	0.613
(0.42)		(52)	(0.14)	(0.32)	(0.034)
11.85	30	599	0.64	3.88	0.587
(0.72)		(52)	(0.17)	(0.38)	(0.038)
15.16	24	643	0.90	3.24	0.509
(0.53)		(54)	(0.16)	(0.27)	(0.036)
18.14	19	693	1.03	2.68	0.459
(0.63)		(48)	(0.19)	(0.32)	(0.052)
19.91	31	725	1.14	2.29	0.397
(0.58)		(46)	(0.25)	(0.31)	(0.055)
22.05	17	742	1.25	2.13	0.364
(0.64)		(61)	(0.17)	(0.23)	(0.036)
25.33	25	748	1.35	2.13	0.291
(0.66)		(62)	(0.24)	(0.32)	(0.050)
29.63	33	752	1.35	2.09	0.287
(1.20)		(64)	(0.28)	(0.27)	(0.052)

As shown in Table 1, the critical energy release rate G_f increases with the increase of the moisture content. This phenomenon can be explained by the fact that more fracture energy is needed for a high moisture content in order to completely delaminate the specimen during the crack growth process due to the fiber bridging effect.

Similarly, to the critical cohesive energy G_f, the critical crack opening displacement w_c has a tendency to linearly increase with the moisture content until 22% and then remains stable for higher values of MC. The critical crack opening displacement w_c obtained in this work varies on average from 0.3 to 1.4 mm from dry to wet wood. The tensile strength f_t decreases when the moisture content increases up to 22%, and f_t is stable for higher MC values. This tendency is in agreement with

the results reported in the literature: the wood strength is constant above the fiber saturation point. This can be related to the absorption of the water in the microstructure. The standard deviation of the tensile strength for most of moisture series is around 0.35 MPa while the mean tensile strength f_t is in range of 1.5 to 7.0 MPa as shown in Table 1.

The ratio $G_{f\mu}/G_f$ also decreases with the increase of the moisture content. These results suggest that the micro-cracking energy plays an important role in the cohesive energy at low moisture contents. On the other hand, it can be deduced that the mechanism of the crack bridging (fiber bridging) - the most essential phenomenon at high moisture - can be related to the fracture behavior of fibers which are assumed to be more ductile at high moisture contents.

4 SUBSTRATE MECHANO-SORPTIVE BEHAVIOUR

Under relative humidity variation, wood substrate behaviour is simulated using the 1D mechanosorptive model developed by Dubois et al [6, 9]. The mechanosorptive model uses a coupling between moisture variations and mechanical properties of wood. An attempt to extend the mechano-sorptive behavior with hygro-lock in 3D was proposed (Figure 7).
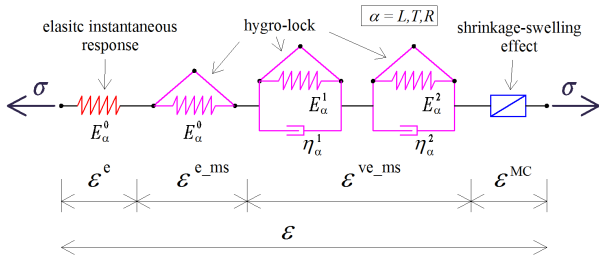

Figure 7: *Mechano-sorptive behavior*

The identification of creep parameters of 3D models for wood is a very difficult task. In spite of the available experimental data on the viscoelastic creep and the mechano-sorptive effect in timber structures, there is still a lack of both experimental work and theoretical background (i.e., the characterization of viscoelastic properties or the Poisson ratios of the orthotropic wood material are depending on the moisture gradients of each orthotropic direction: L-T-R).

Through few experimental tests in literature, viscoelastic creep compliance in the longitudinal direction for 3 different moisture contents for Maritime pine were obtained in Cariou's thesis [2]. In this study, the viscoelastic creep compliance was represented by a simple power law relationship. In order to apply the Kelvin Voigt model, we need to determine the viscoelastic creep compliance coefficients corresponding to Kelvin Voigt model.

We do not know the viscoelastic creep compliance versus moisture for other directions. We assume that the orthotropic factor for all directions is constant at any time and independent of moisture. Based on this assumption, all young moduli, Poisson coefficients, viscosity are depending on the longitudinal viscoelastic properties.

Young moduli and shear moduli versus moisture are obtained from the following expressions (1):

$$\begin{cases} E_T^i(MC) = 0.078.E_L^i(MC) \\ E_R^i(MC) = 0.123.E_L^i(MC) \\ G_{LT}^i(MC) = 0.081.E_L^i(MC) \\ G_{LR}^i(MC) = 0.076.E_L^i(MC) \\ G_{TR}^i(MC) = 0.006.E_L^i(MC) \end{cases} \quad (1)$$

And we also assume that:

$$\eta_R^i(MC) = \eta_T^i(MC) = \eta_L^i(MC) \quad (2)$$

where i denotes the element of the generalized Kelvin Voigt model (i = 0, 1 or 2).

The viscoelastic properties used in the L direction are expressed in Equation 3:

$$\begin{cases} E_L^0(MC) & = 1,35.10^4\,[1.-0,015(MC-12)] \\ E_L^1(MC) & = 1,09.10^5\,[1.-0,024(MC-12)] \\ E_L^2(MC) & = 6,01.10^4\,[1.-0,039(MC-12)] \\ \eta_L^1(MC) & = 6,27.10^6\,[1.+0,004(MC-12)] \\ \eta_L^2(MC) & = 6,92.10^4\,[1.+0,012(MC-12)] \end{cases} \quad (3)$$

The shrinkage-swelling deformations can be expressed as :

$$\Delta\varepsilon_\beta^{MC} = \alpha_\beta.\Delta MC \ \ with \ \beta = L, T \ or \ R \quad (4)$$

The coefficients used in Equation (4) are those reported by Guitard [7]: α_L = 0.005%/%, α_T = 0.32%/%, α_R = 0.19%/%.

In the Husson and Dubois's model, the hygro-lock model is applied for all springs in a generalized Kelvin Voigt model as shown in Figure 7. The elastic stiffness E_α^i of the spring exclusively (without lock) depends on the moisture content and not on its variations. During drying period, the stiffness without lock increasing but the deformation is frozen. The lock effect on the evolution of the stiffness is represented on Figure 8.
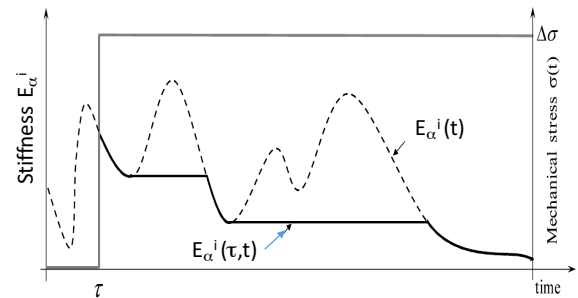

Figure 8: *hygro-lock behaviour; Full line: stiffness evolution with hygro -lock, dash line stiffness evolution without hygro – lock (i=0,1 or 2 and α= L, T or R)*

5 MOISTURE DISTRIBUTION IN THE WOOD SUBSTRATE

A diffusion model based on Fick's second law is applied to obtain the moisture diffusion in wood subtract. In our study, we assume that the surface moisture content of the specimen is at the equilibrium state given by sorption isotherm curve (RH-MC) and that the surface emission coefficients are similar for the three directions (longitudinal, tangential and radial).

In the present work, wood is assumed to follow the Fick's law for the moisture transfer and the temperature is considered to be constant. The second Fick's law is written as:

$$\frac{\partial MC}{\partial t} = \nabla([D].\nabla MC) \qquad (5)$$

where $[D]$, is the second-order diffusion (diagonal) tensor of the moisture transfer, function of MC.

According to Perrée et al. [11], the hydric convection between the above mass transfer coefficient and surface emission coefficient based on the analogousness of the flux for the different potentials can be expressed as:

$$-[D].\nabla MC.\vec{n} = \left(MC_{surf} - MC_{eq}\right).S \qquad (6)$$

where S is the surface emission coefficient (here taken equal to 1.8E-7 m/s). MC_{surf} is the moisture content at the wood surface. MC_{eq} is the equilibrium moisture of wood corresponding to the environment humidity obtained from the sorption isotherm of wood (e.g., Maritime pine) [10].

$$D_\alpha(MC) = D_\alpha^o.e^{k^o MC} \text{ with } \alpha = L, T \text{ or } R \qquad (7)$$

For the three orthotropic directions, values of diffusion coefficients $D\alpha$(MC) (Equation (7)) are obtained from Agoua and Perrée [1] by fitting experimental results. The non linear moisture diffusion coefficient k^o for the absorption and the desorption phases is obtained from Herritsich's work on Radiata pine [8] because k^o is unknown for Maritime pine; Radiata pine and Maritime pine have quite similar characteristics. The Table 2 summarizes the diffusion coefficients used in this study.

Table 2: *Diffusion coefficients used in this study*

	Unit	Long.	Tang.	Radial
D^o	m^2/s	23.2E^{-10}	2.87E^{-10}	4.08E^{-10}
κ^o Absorption	-	3.7	1.64	1.97
κ^o Desorption	-	9.2	6.58	5.95

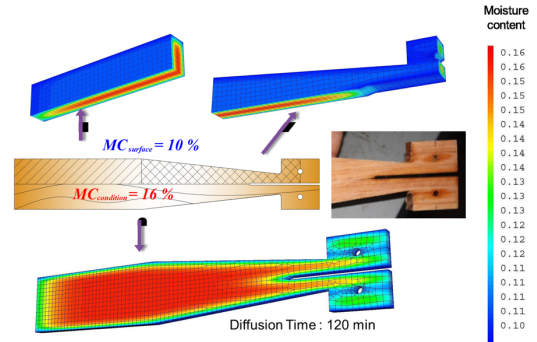An example of moisture distribution obtained are presented on Figure 9.

Figure 9: *Moisture field obtained by diffusion after 120 min*

During the crack propagation, boundary of the moisture surface exchange change, also specimen is remeshing and then projection of the hygro-thermal field before the crack propagation is realised on the new geometry (with the new crack length). At the beginning of the current step, the moisture content field of the specimen is obtained; and then, elastic properties depending on the moisture are updated.

6 INTEGRATION OF MOISTURE VARIATION ON THE COHESIVE ZONE

The crack bridging phenomenon taking place on the FPZ increases the exchange surface and leads the mechanical equilibrium of FPZ to be dependent of the sudden RH variations. Such a phenomenon is expected to be the source of instability of the main crack even if the external loading remained unchanged.

6.1 First adding step

To integration the moisture effect on the fracture process zone, we first suppose that, when the crack propagates under varying moisture, the traction-separation law (TSL) of the new damaged zone is directly function of the moisture at the tip of the FPZ. The cohesive parameters for a given moisture content is estimated on the basis of an interpolation of two experimental values corresponding to two nearest moisture content (upper and lower MC). This TSL law for the new damaged zone does not change for next processes of crack growth (Figure 10) [12].
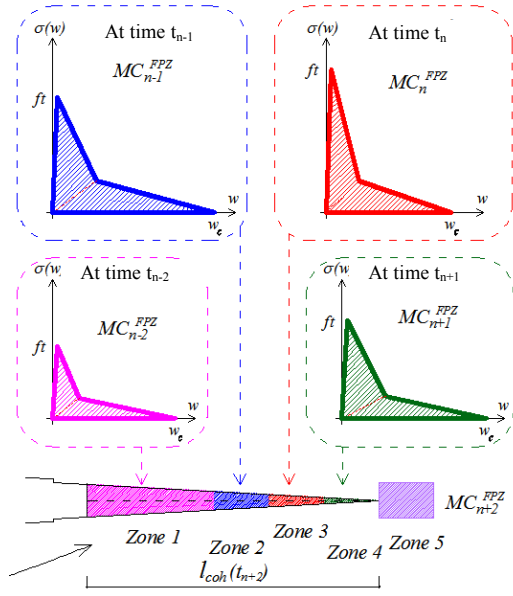
Figure 10: Cohesive law distribution during the crack propagation under varying MC.

6.2 Second adding step: rapid varying moisture effect

Secondly, we propose a method taking into account the rapid varying moisture effect on the FPZ by introducing an additional climatic loading (additional stress field) along the cohesive zone. This additional stress field depends on the moisture in the joint and on the sudden RH variation but also on the stress and on the crack opening state.

The moisture distribution along the cohesive zone is assumed to be weighted by a function $f(w)$ as shown in Figure 11 [12].
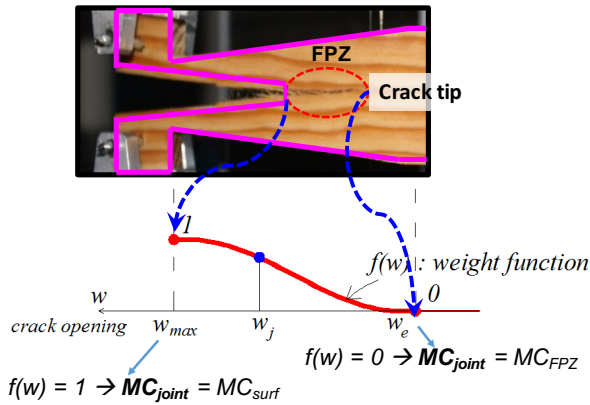

Figure 11: Moisture distribution on the FPZ.

At the beginning of a current computation time t_{n+1}, the moisture content field of the specimen is calculated by the diffusion process in the previous step MC_n and the moisture distribution on the cohesive zone $MC_{joint,n}(w)$ is then obtained.

In order to introduce the additional incremental climatic stress field along the cohesive zone during $\Delta t_n = (t_{n+1}-t_n)$, due to the rapid variation of the moisture, the opening field w along the cohesive zone is considered constant;

the damage d of each joint element is assumed to be independent of the moisture variation. Then, the varying moisture only influences the elastic stiffness of the joint element (damaged fiber). In the cohesive element, the normal stress is a function of the initial elastic stiffness K_o, the damage state d and the crack opening w at the joint element. This relation can be expressed as

$$\sigma = K_o(1-d).w \qquad (8)$$

Thus, the stress at the $j°$ joint element of cohesive zone corresponding to the moisture content $MC_{j,n}$ can be written as :

$$\sigma_j(MC_{j,n}) = K_j(MC_{j,n}).w_j = K_o(MC_{j,n}).(1-d_j).w_j \qquad (9)$$

while the stress corresponding to the new moisture $MC_{j,n+1}$ should be:

$$\sigma_j^*(MC_{j,n+1}) = K_j(MC_{j,n+1}).w_j = K_o(MC_{j,n+1}).(1-d_j).w_j \qquad (10)$$

where K_j is the joint stiffness at the the $j°$ joint element corresponding to the damaged state d_j.

Due to the rapid moisture variation from $MC_{j,n}$ to $MC_{j,n+1}$ at the $j°$ joint element, the perturbation $\Delta\sigma_{j,n}^*$ of the stress corresponding to this variation can be obtained as (d_j and w_j are supposed constants):

$$\Delta\sigma_{j,n}^* = \sigma_j^*(MC_{j,n+1}) - \sigma_j(MC_{j,n}) \qquad (11)$$

$$\Delta\sigma_{j,n}^* = \left(\frac{K_o(MC_{j,n+1})}{K_o(MC_{j,n})} - 1\right).\sigma_j(MC_{j,n}) \qquad (12)$$

with

$$K_o(MC_{j,n}) = \left(1 - a_T.(MC_{j,n} - 12\%)\right).K_o(12\%) \qquad (13)$$

with $a_T = 0,03\%/\%$ in the tangential direction [7].

$$\Delta\sigma_{j,n}^* = \left(\frac{-a_T.(MC_{j,n+1} - MC_{j,n})}{\left(1 - a_T.(MC_{j,n} - 12\%)\right)}\right).\sigma_j(MC_{j,n}) \qquad (14)$$

$$\Delta\sigma_{j,n}^* = A_{j,n}.\sigma_j(MC_{j,n}) \qquad (15)$$

The perturbation stress $\Delta\sigma_{j,n}^*$ due to rapid varying moisture is considered as an external climatic loading applied along the cohesive zone.

Based on Equations (14) and (15), for a humidification phase at the joint, the value of $A_{j,n}$ is negative, and hence the additional stress has the tendency to induce the crack closure. Conversely, for a drying phase at the joint, the value of $A_{j,n}$ is positive and the additional stress has the tendency to lead to additional crack opening.

Figure 12 presents the additional moisture stress $\Delta\sigma_{j,n}^*$ on the FPZ used to integrate the effect of the rapid varying moisture.
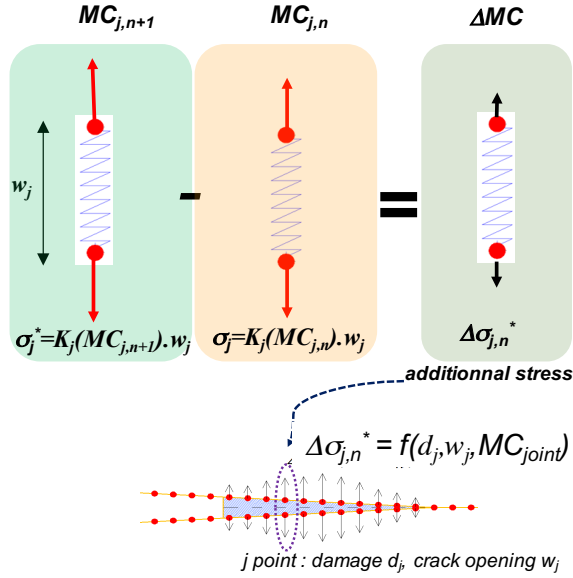
$MC_{j,n+1}$ $MC_{j,n}$ ΔMC

w_j

$\sigma_j^* = K_j(MC_{j,n+1}).w_j$ $\sigma_j = K_j(MC_{j,n}).w_j$ $\Delta\sigma_{j,n}^*$

additionnal stress

$\Delta\sigma_{j,n}^* = f(d_j, w_j, MC_{joint})$

j point : damage d_j, crack opening w_j

Figure 12: *Additional moisture stress ($\Delta\sigma_{j,n}^*$) at the joint j*

7 CRACK GROWTH SIMULATION

The calculations have been implemented in a finite element code (Cast3M). For the wood substrate, the viscoelastic mechano-sorptive behaviour with swelling is the one presented in Section 4. In case of varying moisture in wood, the relation between mechanical properties and the moisture are given in Equations (1) and (2) in Section 4.

The fracture of wood is described from cohesive zone model considering the bi-linear softening. The relation between the cohesive law and the moisture is described in Table 1. Note that, the cohesive zone parameters at a given moisture are estimated from a linear interpolation of those previously identified.

Numerical simulations are realised taking into account first only the first adding step in the cohesive law, the simulations are noted sim1. Secondly, the additional moisture stress presented in Section 6 is also introduced, the simulations are noted sim2. The imposed force is around 170 N, corresponding to 85% of the maximal load at the moisture 12%.

Numerical simulations are compared with experimental results (Figure 13) obtained under variable Relative Humidity. The RH varies from 40% to 90% per 12 hours cycles; this RH variation corresponds nearly to 7% to 22% moisture variation at the specimen surface MC_{surf}. The numerical simulation of the cracked structure under RH variations exhibits a strong coupling effect of the viscoelastic mechano-sorptive behavior (associated to shrinkage-swelling effect) and of the rapid varying moisture on the FPZ. This coupling induces the failure of the specimen. Thus, coupling viscoelastic mechano-sorptive behavior, moisture variation on the FPZ with the additional climatic stress plays a major role on the crack growth and cannot be simply considered as the superposition of both phenomena. In this way, such a complex coupling can only be described through a numerical simulation as the one proposed in this study.
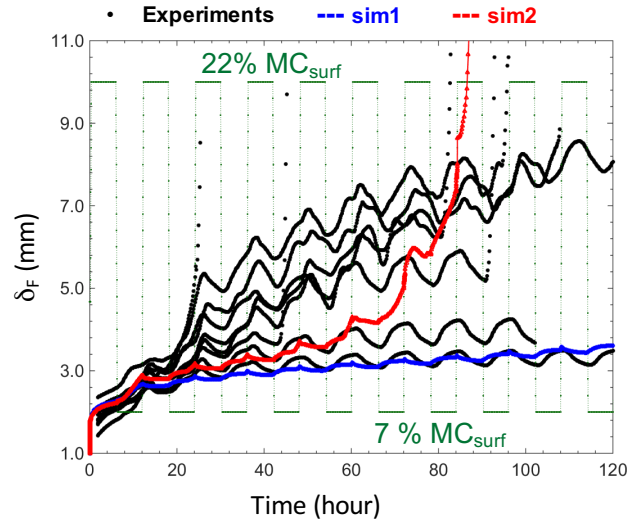

Figure 13: *Load displacement δ_F evolution versus time : experimental results and simulation (sim1 : without additional climatic stress, sim2 : with additional moisture stress on the FPZ). (stress level SL= 0,85%; conditioned moistures MC_{cond}=12%)- Moisture at the wood surface (MC_{surf}) varies between 7% to 22% per 12 hours cycles.*

In Figure 13 a total of 9 experimental curves are presented. The displacement in the experimental test has a tendency to increase versus time due to the viscoelastic properties of wood or to the varying moisture. Moreover, the displacement always evolves with the moisture variation in a moisture cycle (a decrease of the displacement during a humidification phase, and an increase conversely during a drying phase). However, a large scattering of the failure time can be observed from experimental results. Indeed, if the crack appears unstable after 110 hours for most specimens, three of them exhibit an instability after 80 and 100 hours and two specimens failed after 25 hours and 45 hours.

The experimental results appear in agreement with the numerical result obtained on the basis of the complete model (sim2); while the model without the varying moisture effect on FPZ (sim1) only describes the lower experimental response. Some argumentation are proposed in order to explain the difference between the experimental and simulation results. The simulated displacement in Figure 13 cannot be well described due not to only an interpolation of creep compliance in function of the moisture but also to the assumption of the viscoelastic properties for three directions during the simulation. Moreover, the difference may also be related to the diffusion properties which are selected from the literature. Nevertheless, the results could confirm the important role of the coupled effect on the crack growth.

Moreover, as shown in Figure 13, the failure of the specimens occurs during a drying phase. This phenomenon is in agreement with the previous studies

[4]. Note that, we cannot deduce the crack propagation from the displacement of the loading points because it resulted from the coupling between the crack growth (configuration) and the viscoelastic strain in wood; furthermore, this displacement varies depending on the moisture phase (humidification or drying).

8 CONCLUSIONS

A method is proposed in order to analyze the crack growth of timber structures under environmental conditions in which moisture effect is integrated into the fracture Process Zone (FPZ), and leads to express the coupling between the Thermo-Hydro-Mechanical behavior of wood and the crack growth process.

The results obtained from the complete model (sim2: hygro-lock effect associated to the shrinkage-swelling and the rapid varying moisture effect on the FPZ) and the model without varying moisture effect on the FPZ (sim1) are then compared to the experimental ones performed from mTDCB specimens for various conditioned moistures and different stress levels. Despite a large scattering of the experimental results, the numerical simulations sim2 seems to capture the outline of the experimental responses and especially the sudden change of crack growth leading to early failures. The comparison with the numerical results sim1 obtained on the basis of the alone hygro-lock phenomenon emphasize the necessity to consider the instantaneous varying moisture effect on the cohesive zone. The coupling seems to be the key of relevant description of the experimental responses but such a complex coupling, which is not a simple superposition problem, can be described only through a numerical approach as the one proposed in this paper.

Nevertheless, the present numerical model requires other validation procedures and especially a comparison to experimental results of crack growths obtained from more complex RH variations where the magnitudes of the drying phase are different from those of the humidification ones.

REFERENCES

[1] Agoua, E., Zohoun, S., and Perrée, P. A double climatic chamber used to measure the diffusion coefficient of water in wood unsteady-state conditions: determination of the best fitting method by numerical simulation. *Int. J. Heat Mass Transf.* 44: 3731–3744, 2001

[2] Cariou, J.-L. Caracterisation d'un materiau viscoelatisque anisotrope: le bois. PhD thesis, Universite de Bordeaux 1, 1987.

[3] Bazant ZP, Planas J. Fracture and size effect in concrete and other quasibrittle materials. CRC Press, 1998.

[4] Chaplain M, Valentin G. Effects of relative humidity conditions on crack propagation in timber: experiments and modelling. *World Conf. Timber Eng., Auckland, New Zeeland*, 8p, 2010.

[5] Morel S, Lespine C., Coureau J.L., Planas J., Dourado N. Bilinear softening parameters and equivalent LEFM R-curve in quasi-brittle failure, *International Journal of Solids and Structures*, 47 (6): 837–850, 2010.

[6] Dubois F, Husson J-M, Sauvat N, Manfoumbi N., Modeling of the viscoelastic mechano-sorptive behavior in wood. *Mech Time-Dependent Material*, 16:439–460, 2012.

[7] Guitard, D. Mecanique materiau bois et composites. CEPAD, 1987.

[8] Herritsch, A. Investigations on wood stability and related properties of radiata pine. PhD thesis, University of Canterbury, 2007

[9] Husson, J.-M., Dubois, F., and Sauvat, N. A finite element model for shape memory behavior. *Mech. Time-Dependent Mater.* 15(3):213–237, 2001.

[10] Lasserre, B. Modélisation thermo-hygro-mécanique du comportement différé de poutres de structure en bois. PhD thesis, Université de Bordeaux 1, 2000.

[11] Perée, P., and Degiovanni, A. Simulation par volumes finis des transferts coupées en milieux poreux anisotropes : séchage du bois à basse et à haute température. *Int. J. Heat Mass Transf.* 33 (11): 2463–2478,1990.

[12] Phan, N.A, PhD thesis, University of Bordeaux, 2016.

[13] Phan, N. A., Chaplain, M., and Morel, S. Wood moisture content influence on R-curve and on parameters of cohesive zone model. *20th European Conference on Fracture,* 6p, 2014.

[14] Phan N.A., Morel S., Chaplain M. Mixed-mode fracture in a quasi-brittle material: R-curve and fracture criterion – Application to wood. *Engineering Fracture Mechanics* 156 (96) : 113, 2016.